

HIGH-TEMPERATURE LOW-CYCLE FATIGUE OF A MARTENSITIC STAINLESS STEEL. NEW DAMAGE MODEL, APPLIED TO THERMAL FATIGUE

Gérard Degallaix, Jacques Foct *

Strain-controlled low-cycle fatigue tests of a 12 Cr martensitic stainless steel were performed in the temperature range from 350°-600°C. This steel is characterized by a cyclic softening and, for $\Delta\epsilon_p < 2\%$, the factors governing the damage are mainly the plastic strain range and the temperature. A damage law, taking into account a thermally - activated and an athermal plastic flow, is developed. Application to thermal fatigue life prediction is proposed.

INTRODUCTION

Thermal fatigue life prediction involves results of thermal-mechanical tests. These now can be carried out on electrohydraulic machines where both the strain and the temperature are controlled. Generally, the damage per cycle is determined on stabilized hysteresis loops - stress-strain or strain-temperature - by a cumulative damage rule in isothermal fatigue and/or creep. This method may be based on a linear (Spera (1), Chaboche and Stoltz (2), Halford and Manson (3)) or non-linear interaction (Lemaitre and Chaboche (4)) or on equivalent temperature concept (Taira (5)). This implies that, for a given value of $\Delta\epsilon_p$, an isothermal fatigue test leads to the same fatigue life as the thermal testing. There also, calculations use the linear damage rule whose validity under varying temperature has been roughly verified ((5), Rémy et al (6)). At relatively low temperatures, i.e. creep is not predominant, nonetheless Taira observed satisfying correlation on steels. If microstructural transformations do not occur and initiation mechanisms are the same, isothermal and thermal fatigue behaviors can be linked. However, only few studies dealt with the description of isothermal low-cycle fatigue at various temperatures, then applicable to thermal fatigue.

MATERIAL AND EXPERIMENTAL PROCEDURE

The material investigated is a 12 Cr martensitic stainless steel. The chemical composition (wt pct) is 0.2 C, 10.9 Cr, 0.9 Mo, 0.6 Ni,

* Université des Sciences et Techniques de Lille - Laboratoire de Métallurgie physique Bât.C6-59655 Villeneuve d'Ascq Cedex - France

0.3 V, 0.6 Mn, 0.2 Si. The samples have been air quenched from 1050°C and tempered for two hours at 760°C.

Tensile and fatigue tests were carried out at various temperatures in the range from 350°-600°C, especially at the upper and lower limits of this range. Cylindrical specimens having threaded ends and a diameter of 10 mm over the reduced gauge length were employed. Experiment was conducted on a 400 kN servohydraulic push-pull MTS machine, equipped with a diametral extensometer and an infrared furnace. Total longitudinal strain control with the commonly used triangular waveshape (strain rate : $4 \times 10^{-3} \text{ s}^{-1}$) was chosen. Details of the test procedure and of the results have been given elsewhere (Degallaix et al (7)).

EXPERIMENTAL RESULTS

This material is characterized by a cyclic softening concerning as well the comparison between the cyclic and monotonic stress-strain relations as the stress evolution along the tests. This tendency seems to be common for the martensitic stainless steels and could be explained by the important dislocation density due to the martensitic transformation which induces high initial flow stress. This has been observed in other 12 Cr steels (Kanazawa et al (8)). Fig. 1 summarizes our results at 350° and 600°C.

Except a very slight hardening at 350°C, during less than 2 % N_R , stress amplitude decreases with increasing strain cycles for all test conditions. This is more marked with increasing temperature or strain amplitude. While strain hardening exponent is independent of test temperature (monotonic : 0.10, cyclic : 0.13), we observe a fall of the 0.2 % yield strength, from static to dynamic (10 % at 350°C, 30 % at 600°C). See Fig. 1.

In the high strain range ($\Delta\epsilon_t > 2\%$) fatigue life is relatively independent of test temperature. When $\Delta\epsilon_t$ becomes lower, and for a given value, life decreases on increasing the test temperature from 350° to 600°C, this becomes all the more significant as $\Delta\epsilon_t$ decreases. So the fatigue life ratio between 350° and 600°C equals 1 for $\Delta\epsilon_t = 2\%$, 1.9 for $\Delta\epsilon_t = 1\%$ and 4.6 for $\Delta\epsilon_t = 0.5\%$.

Manson-Coffin lines ($\Delta\epsilon_p$ versus N_R) are shown in Fig. 2.

Within our experimental conditions, the parameters which control damage are mainly plastic strain range and temperature. We have observed that the damage process is primarily a function of plastic strain range at low fatigue life, while at high fatigue life, it is strongly dependent on test temperature. Moreover, the greater $\Delta\epsilon_p$, the less T has an effect. Then it seems that the fatigue damage is here simultaneously governed by two kinds of mechanisms dependent on the plastic strain range, thermally activated or athermal.

So, we fit the damage with the following relation (Degallaix et al (9)).

$$\frac{1}{N_R} = A_1 \cdot \Delta\epsilon_p^{b_1} \cdot \exp\left(-\frac{Q}{RT}\right) + A_2 \cdot \Delta\epsilon_p^{b_2} \quad (1)$$

Constants A_1 , b_1 , A_2 , b_2 and apparent activation energy Q are material constants in the range of this study. Their values, obtained with a computer code, are $A_1 = 17350 \times 10^{-5}$, $b_1 = .692$, $Q = 12.24$ kcal/mole, $A_2 = 63 \times 10^{-5}$, $b_2 = 1.91$. So, the thermally-activated term have a much smaller plastic strain range sensitivity than the athermal term.

High temperature fatigue life results from various processes. To our knowledge, no clear relation between an apparent activation deduced from $N_R(T)$ and the energies associated to simple phenomena has been proposed. It is generally observed that damage processes do not seem to be activated when environmental effects are removed (Coffin (10)). So, the activated term may be provided from air experiment. Otherwise, homogeneity of the plastic flow is an important microscopic factor. This homogeneity, which increases fatigue life, is enhanced by the three dimensional dislocation array in cell structure. Such a cell structure is mainly due to the processes of climb and cross slip dislocations which are thermally activated. In other 12 Cr steels, this kind of array has been observed (8).

In any way, the thermal activated part in the damage per cycle is here increasing from 2 to 25 % for $\Delta\epsilon_p = 0.8$ %, and from 10 to 64 % for $\Delta\epsilon_p = 0.2$ %, when T rises from 350° to 600°C.

Fatigue life curves described by eq. (1) are also shown in Fig. 2. Lives estimated by the six Manson-Coffin equations or by the proposed model correlate very well all the data that were obtained up to $\Delta\epsilon_t = 2$ %. A life-factor of 1.6 (1.15 on the average) is observed, which is very satisfying considering the experimental scattering inherent in fatigue phenomena (9). Moreover, we can define simply low-cycle fatigue behavior of this material by a strength surface represented Fig. 3.

APPLICATION TO THERMAL FATIGUE

In order to evaluate the damage progress in a thermal fatigue test, carried out in the same frequency range, we shall argue with Taira's assumptions (5), in particular the linear damage rule. In the further discussion, we consider the damage per cycle $\Delta\phi = 1/N_R$, or more precisely, the damage per half cycle $\Delta\phi = 1/2 N_R$.

From eq. (1), it is clear that in an isothermal fatigue test and during each half cycle, plastic strain $\delta\epsilon_p$ changes from the value 0 to $\Delta\epsilon_p$ and damage $\delta\phi$ from 0 to $\Delta\phi$ as :

$$\delta\phi = \frac{A_1}{2} \delta\epsilon_p^{b_1} \exp\left(-\frac{Q}{RT}\right) + \frac{A_2}{2} \delta\epsilon_p^{b_2} \quad (2)$$

Although eq. (2) describes originally isothermal damage, it is assumed that this equation is applicable to thermal fatigue in which the variation of T has to be considered. Then the increment of damage $d(\delta\phi)$, connected with the increments of plastic strain $d(\delta\epsilon_p)$ and of temperature dT , is given, differentiating eq. (2) by :

$$d(\delta\phi) = \left[\frac{A_1 b_1}{2} \delta\epsilon_p^{b_1-1} \exp\left(-\frac{Q}{RT}\right) + \frac{A_2 b_2}{2} \delta\epsilon_p^{b_2-1} \right] d(\delta\epsilon_p) + \left[\frac{A_1}{2} \delta\epsilon_p^{b_1} \frac{Q}{RT^2} \exp\left(-\frac{Q}{RT}\right) \right] dT \quad (3)$$

With numerical values ϵ_p and T taken on the stabilized hysteresis loop, the integration of eq. (3) allows the damage evaluation during the heating ($T_1 \rightarrow T_2$) and cooling ($T_2 \rightarrow T_1$) paths. A representation of idealized loops is given Fig. 4 for a typical thermal-mechanical fatigue test with external constraint (Coffin-type test). Then the thermal fatigue damage per cycle, i.e. :

$$\Delta\phi [T_1 \rightarrow T_2] = \Delta\phi [T_1 \rightarrow T_2] + \Delta\phi [T_2 \rightarrow T_1] \quad (4)$$

gives an estimation of the fatigue life. By using eq. (1), parameters $\Delta\epsilon_p$ and T of equivalent isothermal tests can be determined.

Though this analysis relating isothermal fatigue to thermal fatigue is, of course, not complete, it offers a simple approach to solve practical problems.

CONCLUSION

We describe the behavior of a 12 Cr martensitic stainless steel in high temperature isothermal low-cycle fatigue. We develop a damage model in terms of plastic strain range and temperature which points out a thermal activation. For thermal-mechanical fatigue tests a method is detailed to estimate fatigue life and to characterize equivalent isothermal tests.

ACKNOWLEDGMENT

The authors wish to express their appreciation to A.Vanderschaeghe, Chief Engineer, and C. Gabrel, Stein-Industrie, for their support in experiments.

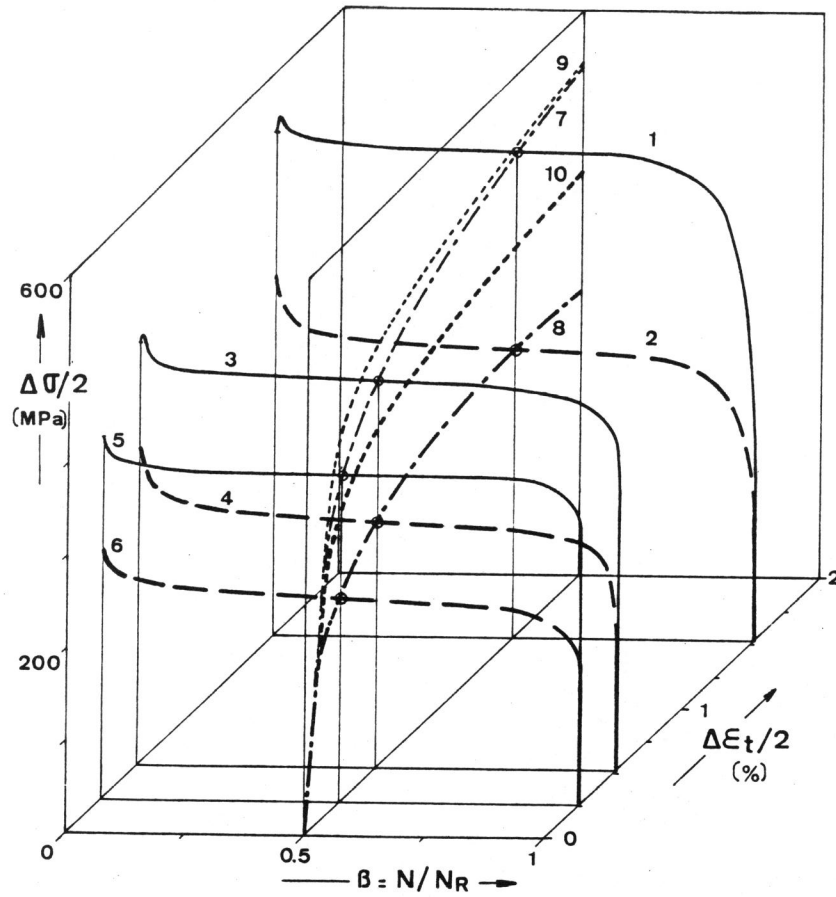
SYMBOLS USED

- A_1 = material constant
- A_2 = material constant
- b_1 = material constant
- b_2 = material constant
- N = number of cycles
- N_R = number of cycles to failure
- Q = apparent activation energy (kcal/mole)
- R = gas constant ($2 \cdot 10^{-3}$ kcal/mole \times K)
- T = temperature ($^{\circ}$ C, $^{\circ}$ K in the eq. 1-4)

- β = cycle ratio, $\beta = N/N_R$
 $\Delta\epsilon_t$ = total strain range (%), $\Delta\epsilon_t/2$ strain amplitude (%)
 $\Delta\epsilon_p$ = plastic strain range (%)
 $\Delta\sigma/2$ = stress amplitude (MPa)
 $\Delta\phi$ = damage per cycle
 $\Delta\psi$ = damage per half cycle

REFERENCES

1. Spera, D.A., 1973, ASTM, STP 520, 648.
2. Chaboche, J.L., and Stoltz, C., 1974, Rev. Fr. Méca., 52, 37.
3. Halford, G.R., and Manson, S.S., 1976, ASTM, STP 612, 239.
4. Lemaitre, J., and Chaboche, J.L., 1974, Symp. IUTAM, Onera, T.P. 1394.
5. Taira, S., 1973, ASTM, STP 520, 80.
6. Rémy, L., Reuchet, J., Thiery, J., and Herman, C., 1980, Report D.G.R.S.T., n° 78-7-2437.
7. Degallaix, G., Foct, J., Gabrel, C., and Vanderschaeghe, A., 1982, Mém. Sc. Rev. Mét., 79-1, 21.
8. Kanazawa, K., Yamaguchi, K., and Kobayashi, K., 1979, Mat. Sc. Eng., 40, 89.
9. Degallaix, G., Degallaix, S., and Foct, J., to be published in Mat. Sc. Eng.
10. Coffin, L.F., 1972, Met. Trans. A., 3, 1777.



	Temperature T (°C)	350	600
stress amplitude - cycle ratio curves	$\Delta\epsilon_t/2 = 1.53\%$	— 1	- - - 2
	$\Delta\epsilon_t/2 = 0.52\%$	— 3	- - - 4
	$\Delta\epsilon_t/2 = 0.26\%$	— 5	- - - 6
stress - strain curves	cyclic	- - - 7	- - - 8
	monotonic	- - - - 9	- - - - 10

Figure 1 Cyclic softening of the material

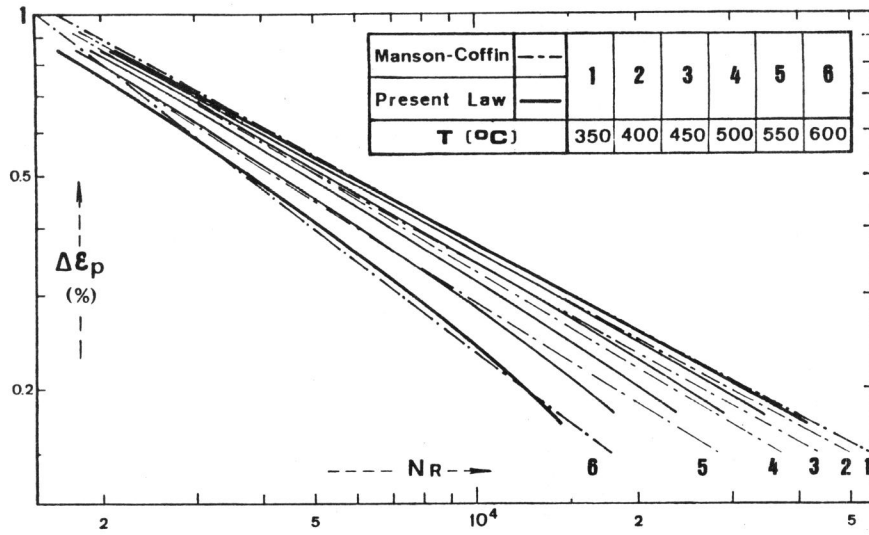


Figure 2 Plastic strain range-life curves as a function of temperature

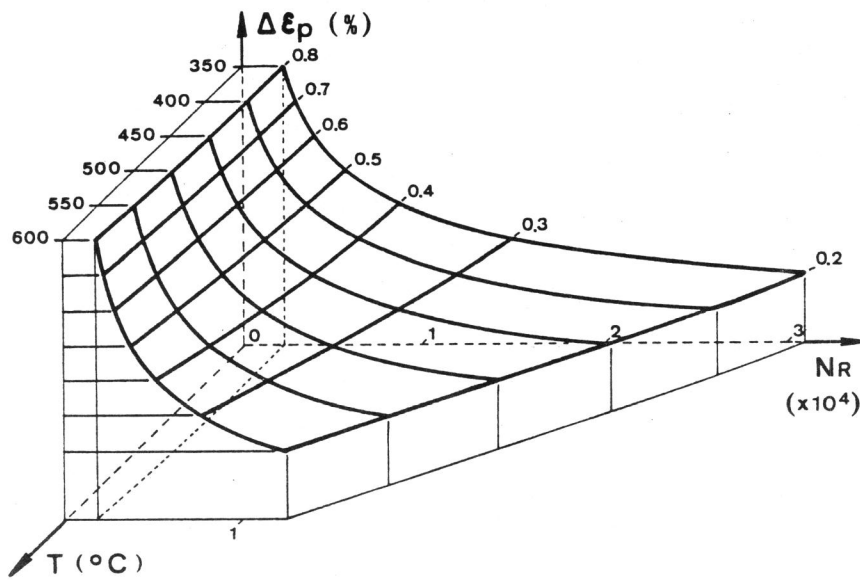
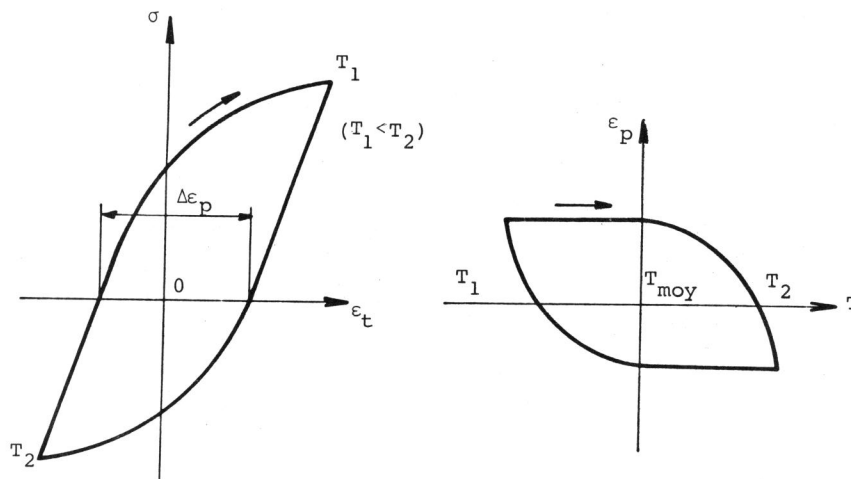


Figure 3 Fatigue strength surface defined by the proposed damage law



(a) stress σ - total strain ϵ_t (b) plastic strain ϵ_p - temperature T

Figure 4 Idealized hysteresis loops (thermal-mechanical Coffin - type test)